

## THE ENIGMATIC PAIR OF DWARF GALAXIES LEO IV AND LEO V: COINCIDENCE OR COMMON ORIGIN?

JELTE T. A. DE JONG<sup>1</sup>, NICOLAS F. MARTIN<sup>1</sup>, HANS-WALTER RIX<sup>1</sup>, KESTER W. SMITH<sup>1</sup>, SHOKO JIN<sup>2,3</sup>, ANDREA V. MACCIÒ<sup>1</sup>

*Draft version November 4, 2018*

### ABSTRACT

We have obtained deep photometry in two  $1^\circ \times 1^\circ$  fields covering the close pair of dwarf spheroidal galaxies Leo IV and Leo V and part of the area in between. From the distribution of likely red giant branch and horizontal branch stars in the data set, we find that both Leo IV and Leo V are significantly larger than indicated by previous measurements based on shallower data. With a half-light radius of  $r_h = 4.6 \pm 0.8$  ( $206 \pm 36$  pc) and  $r_h = 2.6 \pm 0.6$  ( $133 \pm 31$  pc), respectively, both systems are now well within the physical size bracket of typical dwarf spheroidal Milky Way satellites. Both are also found to be significantly elongated with an ellipticity of  $\epsilon \simeq 0.5$ , a characteristic shared by many of the fainter ( $M_V > -8$ ) Milky Way dwarf spheroidals. The large spatial extent of our survey allows us to search for extra-tidal features in the area between the two dwarf galaxies with unprecedented sensitivity. The spatial distribution of candidate red giant branch and horizontal branch stars in this region is found to be non-uniform at the  $\sim 3\sigma$  level. Interestingly, this substructure is aligned along the direction connecting the two systems, indicative of a possible ‘bridge’ of extra-tidal material. Fitting the stellar distribution with a linear Gaussian model yields a significance of  $4\sigma$  for this overdensity, a most likely FWHM of  $\sim 16$  arcmin and a central surface brightness of  $\simeq 32$  mag arcsec<sup>-2</sup>. We investigate different scenarios to explain the close proximity of Leo IV and Leo V and the possible tidal bridge between them. Orbit calculations demonstrate that the two systems cannot share the exact same orbit, while a compromise orbit does not approach the Galactic center more than  $\sim 160$  kpc, rendering it unlikely that they are remnants of a single disrupted progenitor. A comparison with cosmological simulations shows that a chance collision between unrelated subhalos is negligibly small. Given their relative distance and velocity, Leo IV and Leo V could be a bound ‘tumbling pair’, if their combined mass exceeds  $8 \pm 4 \times 10^9 M_\odot$ . The scenario of an internally interacting pair that fell into the Milky Way together appears to be the most viable explanation for this close celestial companionship.

*Subject headings:* galaxies: individual (Leo IV dSph, Leo V dSph) – Local Group

### 1. INTRODUCTION

In the past four years, the Sloan Digital Sky Survey (SDSS) has revealed satellite galaxies of the Milky Way (MW) that are up to 100 times fainter than those known before, more than doubling the number of known satellites. Most of these new discoveries are dwarf spheroidal galaxies (dSph) that are dark-matter dominated objects (Martin et al. 2007; Simon & Geha 2007), yet have surprisingly complex star formation histories (de Jong et al. 2008a) and/or morphologies (e.g. Coleman et al. 2007a; Martin et al. 2008a; de Jong et al. 2008b). Thanks to these new objects and the uniform sky coverage provided by SDSS, it is now possible to probe the faint end of the satellite galaxy luminosity function (e.g. Koposov et al. 2008). This extended data set has enabled a detailed comparison with galaxy formation models, leading to better agreement between models and observation, thereby largely solving the ‘missing satellite problem’, one of the stumbling blocks for current cosmological models on small scales (e.g. Koposov et al. 2009; Macciò et al. 2009). Recent studies of the struc-

tural properties of these newly discovered dwarf galaxies based on SDSS data have revealed that they are, as a class, more elongated than their brighter counterparts (Martin et al. 2008b), indicating that some systems may be tidally disrupted by the MW. It is as yet unclear whether these objects represent a lower mass limit to the galaxy formation process, or whether their stellar bodies are remnants of originally larger systems.

In this context, the recently discovered systems Leo IV (Belokurov et al. 2007) and Leo V (Belokurov et al. 2008) are particularly interesting, as they are separated by less than  $3.0^\circ$  on the sky with fairly similar distances ( $154 \pm 5$  kpc and  $\sim 180$  kpc, respectively; Moretti et al. 2009; Belokurov et al. 2008) and radial velocities ( $10.1 \pm 1.4$  km s<sup>-1</sup> and  $60.8 \pm 3.1$  km s<sup>-1</sup>, respectively, with respect to the Galactic Standard of Rest; Simon & Geha 2007; Belokurov et al. 2008), implying that they might be related to a single disrupting or disrupted progenitor. Belokurov et al. (2008) also found the distribution of blue horizontal branch (BHB) stars in Leo V to be elongated and even detected two candidate red giant branch (RGB) stars at  $\sim 13'$  North of the system, well beyond the estimated tidal radius. Furthermore, with its estimated half-light radius of  $\sim 40$  pc (Belokurov et al. 2008), Leo V appears to fall in the ‘size gap’ between globular clusters and classical dwarf spheroidal galaxies (cf. Gilmore et al. 2007).

We have obtained deep photometry in two  $1^\circ \times 1^\circ$

Electronic address: dejong@mpia.de

<sup>1</sup> Max-Planck-Institut für Astronomie, Königstuhl 17, D-69117 Heidelberg, Germany

<sup>2</sup> Astronomisches Rechen-Institut, Zentrum für Astronomie der Universität Heidelberg, Mönchhofstraße 12-14, D-69120 Heidelberg, Germany

<sup>3</sup> Alexander von Humboldt research fellow

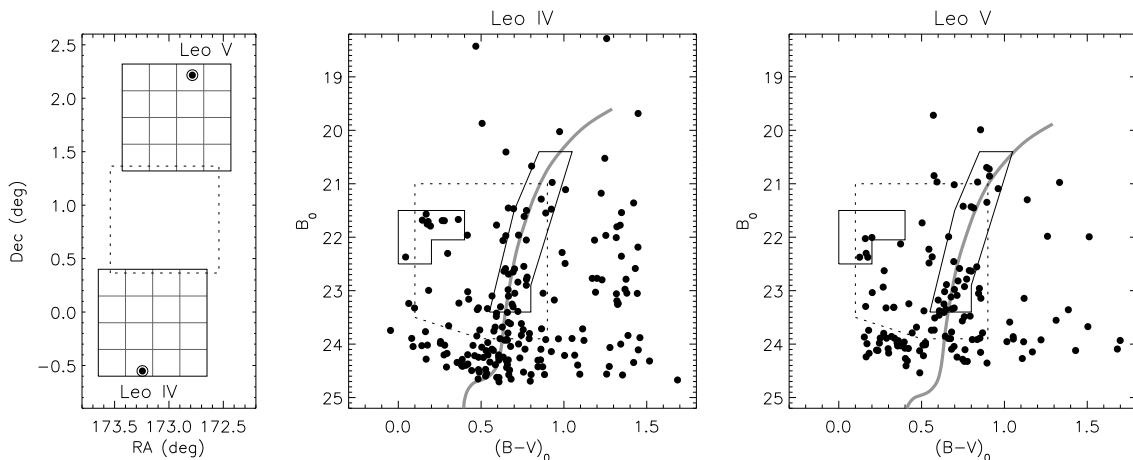


FIG. 1.— Layout of observed fields and color-magnitude diagrams. *Left*: Black solid lines outline the two  $1^\circ \times 1^\circ$  fields that were obtained, with the gray lines showing the individual chips. The dashed square outlines the third field that was lost to bad weather. The locations of Leo IV and Leo V are indicated. *Middle*: Color-magnitude diagram of Leo IV within  $3'$  from the center. Overplotted is a 14 Gyr isochrone with  $[\text{Fe}/\text{H}] = -2.3$  and  $m - M = 20.94$ . Two selection boxes to select HB and RGB stars are shown with solid outlines, while a third selection box used for the maximum-likelihood fitting procedure is indicated with a dashed outline. *Right*: As the middle panel, but for Leo V. Here the isochrone has  $m - M = 21.23$ . In both cases the isochrones are from Dotter et al. (2008).

fields, covering both Leo IV and V as well as much of the area in between them. These new data enable a re-determination of the structural parameters for both galaxies, as well as a sensitive search for possible extra-tidal material connecting the two systems. The remainder of this paper is structured as follows. In §2 the data and data reduction process are detailed. Revised structural parameters for Leo IV and Leo V are presented in §3. The different ways in which we search for evidence of extra-tidal stars in between the two systems is described in §4, and in §5 several scenarios to explain the relation between them are discussed. A short summary and our conclusions are presented in §6.

## 2. DATA

Deep, wide-field photometry in the Johnson  $B$  and  $V$  filters was obtained for two  $1^\circ \times 1^\circ$  fields, using the LAICA imager on the 3.5m telescope at the Calar Alto observatory. Four  $4\text{k} \times 4\text{k}$  CCDs with a pixel size of  $0''.22$  are positioned such that a mosaic of 4 pointings provides a  $1^\circ \times 1^\circ$  field of view. Observations were carried out during the nights of February 24th and 25th 2009, under photometric conditions with seeing ranging from  $1''.2$  to  $1''.8$ . Total exposure times in  $B$  and  $V$  were 1950s and 2600s, divided over single exposures of 650s. The locations of the fields are shown in the left panel of Figure 1; a planned central field could not be obtained due to bad weather.

After bias subtraction and flatfielding, the data from the individual chips were astrometrically corrected and stacked using the *SCAMP* (Bertin 2006) and *SWARP* software<sup>4</sup>, developed by Terapix. A chip-by-chip analysis of the data was necessary because of seeing differences between different pointings and PSF distortions. Object detection was done using SExtractor (Bertin & Arnouts 1996) and subsequent PSF-fitting photometry with the *daophot* package in IRAF. By cross-matching objects with SDSS DR7 (Abazajian et al. 2009) and converting SDSS magnitudes to  $B$  and  $V$  using the transformations

from Jester et al. (2005), the photometry was calibrated to SDSS. The photometry of all stars is made available in Table 1, which contains the coordinates, magnitudes and their uncertainties, and the extinction at the position of each star interpolated from the extinction maps of Schlegel et al. (1998). Using these extinction values, all stars were individually corrected for the limited foreground extinction towards these fields ( $E(B - V) \sim 0.1$ ). The final calibrated and dereddened magnitudes will hereafter be referred to as  $B_0$  and  $V_0$ . Color-magnitude diagrams (CMD) of Leo IV and V within radii of  $3'$  are presented in Figure 1. Artificial star tests to assess the completeness in all CCDs were done by placing 4500 sources spread over a magnitude range of 17 to 25 in each CCD and for each filter and analysing them following the exact same procedure. The completenesses derived are shown in Figure 2 for the Leo IV field and in Figure 3 for the Leo V field. Seeing variations cause the completeness to be non-uniform, but  $\sim 80\%$  completeness is reached to at least  $B_0 = V_0 \simeq 23.5$  over the whole field, or approximately 1.5 magnitudes fainter than the SDSS.

## 3. REVISED PROPERTIES OF LEO IV AND LEO V

An accurate distance to Leo IV has been determined by Moretti et al. (2009) using RR Lyrae stars. Although the absolute calibration of our photometry would introduce uncertainties in the determination of the distance to Leo V, the luminosity of its HB stars can be compared to the luminosity of the HB in Leo IV, providing a distance offset with respect to the latter. The stars on the horizontal part of the horizontal branch (HB) of Leo IV have a mean  $B_0 = 21.78 \pm 0.06$ , while for Leo V we find  $B_0 = 22.06 \pm 0.04$ . Assuming a distance modulus of  $20.94 \pm 0.07$  ( $154 \pm 5$  kpc, Moretti et al. 2009) for Leo IV, this gives a distance modulus of  $21.22 \pm 0.10$ , or a distance of  $175 \pm 9$  kpc, for Leo V.

Based on our new photometry, we re-determine the structural parameters of the two dwarf galaxies using the algorithm developed and detailed in Martin et al. (2008b). We refer the reader to this paper for details but recall that this maximum likelihood (ML) algorithm uses the spatial positions of stars that are plausible

<sup>4</sup> *SCAMP* and *SWARP* can be obtained from <http://terapix.iap.fr>

TABLE 1  
PHOTOMETRIC DATA

Chip ID*	$\alpha$ ( $^{\circ}$ J2000.0)	$\delta$ ( $^{\circ}$ J2000.0)	$B$ (mag)	$\sigma_B$ (mag)	$V$ (mag)	$\sigma_V$ (mag)	E(B-V) (mag)
0_11	173.33533	2.05084	23.302	0.042	21.902	0.014	0.028
0_11	173.23705	2.05027	23.603	0.048	22.295	0.021	0.028
0_11	173.28453	2.05040	23.531	0.042	23.185	0.047	0.028
0_11	173.29111	2.04999	24.160	0.071	23.551	0.074	0.028
0_11	173.27151	2.05098	23.059	0.028	22.804	0.032	0.028

NOTE. — The complete table is available online.

\* The first digit of the chip ID indicates the field, where a ‘0’ stands for the Northern field containing Leo V and a ‘1’ for the Southern field containing Leo IV; the integers following the underscore signify the exposure and the chip number, respectively, both running from 1 to 4.

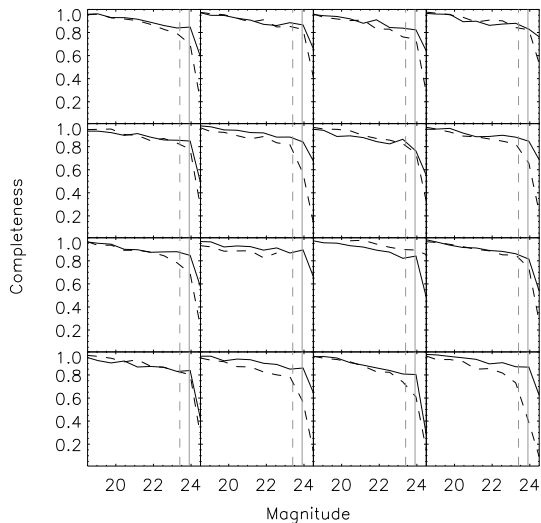


FIG. 2.— Completeness as a function of magnitude for all CCDs in the  $1^{\circ} \times 1^{\circ}$  field containing Leo IV. The solid line is for the  $B$ -band, and the dashed line for the  $V$ -band. Gray vertical lines indicate the magnitude limits used for the maximum-likelihood analysis of the stellar spatial distribution: 23.9 for  $B_0$  (solid) and 23.4 for  $V_0$  (dashed).

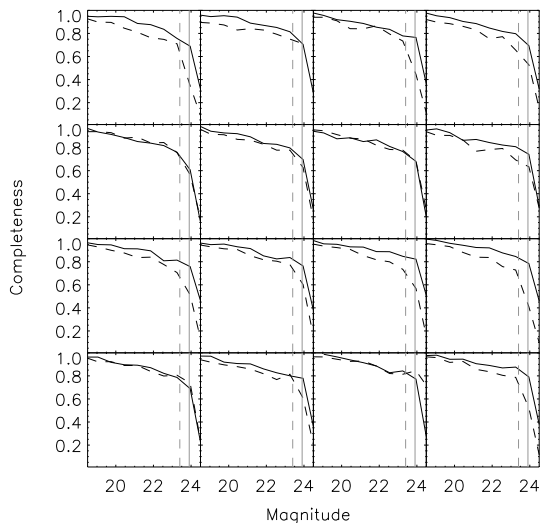


FIG. 3.— As Fig. 2 but for the field containing Leo V.

members of a dwarf galaxy (selected by a rough color-magnitude cut) to determine the best elliptical, exponential surface density profile of the satellite, and fit for the fore/background stars at the same time. Given the positions of Leo IV and V near the edge of the observed fields, we use the adapted version of the algorithm presented in §3.3 of Martin et al. (2009). This version accounts for holes and gaps in data sets by iteratively populating un-observed regions with a stellar density that follows the best model from the previous iteration. The contribution of this stochastic method to the uncertainties on the model parameters is determined via a Monte Carlo approach, in which 100 fits are performed for each galaxy.

The results of the application of the algorithm on the LAICA data are listed in Table 1 and show that both galaxies are quite elliptical, with axis ratios of 2:1. For Leo IV, this value is consistent with the previous measurement based on SDSS data given its large uncertainties, but the ellipticity–half-light radius covariance (see Fig. 9 of Martin et al. 2008b) implies a system that is significantly larger than previously measured. As for Leo V, previous estimates of its properties relied on a circular model and therefore also underestimated its size. With the new measurements, both galaxies have half-light major axes of over 100 pc, removing them from the ‘size gap’ that exists between dwarf galaxies and globular clusters at brighter magnitudes (e.g. Gilmore et al. 2007). The major axes of the systems do not seem in any way correlated with their relative positions. The high ellipticity for Leo IV is, however, different from the results of Sand et al. (2009), who find Leo IV to be very round. Since Sand et al. (2009) use subgiant and main-sequence stars that are below our detection threshold and ignore BHB stars, differences could be caused by morphological differentiations between different stellar populations. The fact that Leo IV and Leo V lie very close to the edge, possibly even partly outside of our surveyed area of view might also influence our measurements in some unforeseen way.

Using the number of stars in each dwarf galaxy, which is an output of the ML algorithm, and assuming a stellar population (in this case old, 14 Gyr, and metal-poor,  $[\text{Fe}/\text{H}] = -2.3$ ), the total luminosities are also derived following the same procedure as in Martin et al. (2008b). The resulting luminosities are  $M_V = -5.8 \pm 0.4$  and  $-5.2 \pm 0.4$  for Leo IV and V, respectively. The revised value for Leo IV is 0.8 magnitudes brighter than the value

TABLE 2  
STRUCTURAL PARAMETERS OF LEO IV AND LEO V

Parameter	Leo IV	Leo V
$\alpha_0$ (J2000)	11 32 58.6 $\pm$ 1.6	11 31 08.4 $\pm$ 1.6
$\delta_0$ (J2000)	-00 33 06 $\pm$ 54	+02 12 57 $\pm$ 12
$\theta$ (deg)	-59 $\pm$ 9	-84 $\pm$ 13
$\epsilon$	0.49 $\pm$ 0.11	0.50 $\pm$ 0.15
$r_h$ (arcmin)	4.6 <sup>+0.8</sup> <sub>-0.7</sub>	2.6 $\pm$ 0.6
$r_h$ (pc)	206 <sup>+36</sup> <sub>-31</sub>	133 $\pm$ 31
$D$ (kpc)	154 $\pm$ 5 <sup>a)</sup>	175 $\pm$ 9
$m - M$ (mag)	20.94 $\pm$ 0.07 <sup>a)</sup>	21.22 $\pm$ 0.10
[Fe/H]	-2.3 $\pm$ 0.1 <sup>a)</sup>	-2.0 $\pm$ 0.2 <sup>b)</sup>
$M_V$	-5.8 $\pm$ 0.4	-5.2 $\pm$ 0.4
$L_V$ ( $L_\odot$ )	1.8 $\pm$ 0.8 $\times 10^4$	1.0 $\pm$ 0.5 $\times 10^4$
$\mu_V$ (mag/arcsec <sup>2</sup> )	27.5 $\pm$ 0.7	27.1 $\pm$ 0.8
$v_{\text{GSR}}$ (km s <sup>-1</sup> )	10.1 $\pm$ 1.4 <sup>c)</sup>	60.8 $\pm$ 3.1 <sup>d)</sup>

NOTE. — <sup>a)</sup>Moretti et al. (2009); <sup>b)</sup>Walker et al. (2009); <sup>c)</sup>Simon & Geha (2007); <sup>d)</sup>Belokurov et al. (2008); all other values based on this publication.

from Martin et al. (2008b), but they agree to within  $1\sigma$ . It is also statistically equivalent to the value measured by Sand et al. (2009) from their deeper data. The difference is due to the fact that the deeper data reveal that Leo IV is actually more elongated and has a larger half-light radius than that measured from SDSS data. Leo V is found to be almost a magnitude brighter than the lower limit given by Belokurov et al. (2008), who only took into account the light inside an aperture of  $3'$ .

#### 4. A BRIDGE OF STARS BETWEEN LEO IV AND LEO V?

At the Galactic latitudes where Leo IV and V are located,  $b \sim 50^\circ$ , the Galactic stellar populations do not vary significantly. Hence, in the absence of tidal features related to Leo IV and/or Leo V the spatial distribution of stars, in any region of the color-magnitude plane, is expected to be very close to uniform in the area between the two galaxies. We define a coordinate system  $(X, Y)$ , rotated with respect to  $(\alpha, \delta)$ , such that Leo IV is located at the origin and Leo V lies along the  $Y$ -axis. Using the color-magnitude selection boxes overplotted on the CMDs in Figure 1, candidate HB and RGB stars at the distance of Leo IV and V are selected. Their spatial distributions in the  $(X, Y)$  coordinate system are shown in Figure 4. The magnitude limit of  $B_0 < 23.5$  ensures that no systematic completeness biases affect these distributions (see Fig. 3 and 2). Leo IV and Leo V are visible as overdensities at the very bottom and top of the field. The flattening of Leo IV is also apparent from the contours showing the RGB star density, consistent with our structural parameter estimates. However, no obvious extra-tidal features are visible.

As a sensitive test for a possible overdensity of extra-tidal stars between the two dwarf galaxies, we divide the observed field in  $0.2^\circ$ -wide bins along the  $X$ -axis. In the following analysis we exclude all data within 5 half-light radii of the dwarf galaxies (the ellipses in Fig. 4). The combined density of RGB and HB stars in each bin is plotted in panels (a) to (c) of Figure 5 with filled circles for the individual mosaics and the complete data set. The same is done for MW foreground M dwarf stars (selected in the color-magnitude region  $21.0 < B_0 < 23.5$ ,

$1.1 < B_0 - V_0 < 1.6$ ) and plotted with open squares. Similar  $0.2^\circ$ -wide bins are defined along the  $\delta$ -axis and their stellar densities are shown in panel (d). The distribution of MW foreground stars is consistent with being uniform, both in  $X$  and in  $\delta$ . In contrast, the RGB and HB stars are uniformly distributed in  $\delta$ , but not in  $X$ , where in both fields substructure is visible that resembles a bump or overdensity at  $X \sim -0.1^\circ$ . Based on basic Poisson statistics the significance of this bump is approximately  $3.5\sigma$ . Kolmogorov-Smirnov (KS) tests (Press et al. 1992) indicate that the probability of the distribution of RGB and HB stars along the  $X$ -axis being drawn from a uniform distribution is only 0.4%, thus rejecting this null hypothesis at the  $\sim 3\sigma$  level. Along the  $\delta$ -axis this probability is 56%, and for the MW foreground stars the probabilities are 87% and 62% respectively, thus all consistent with a uniform distribution. Both tests therefore indicate the presence of substructure only in the distribution of RGB and HB stars and only along the direction parallel to a line connecting Leo IV and V. In addition, the KS test also shows that the distributions of RGB and HB stars along the  $X$ -axis in the individual fields are consistent with being drawn from the same distribution, with a probability of 59%. The substructure is therefore not isolated to a single field.

To estimate the significance of this overdensity rigorously, we performed a ML fit similar to the one used to determine the structural parameters of the galaxies. The density at any point  $(X, Y)$  of the field of view,  $\Sigma(X, Y)$ , is here modeled by a flat background,  $\Sigma_b$ , with an additional linear enhancement that is constant along the Leo IV/V axis (the  $Y$ -axis of Fig. 4) and of Gaussian form  $G(X|A, X_0, \sigma)$  along the  $X$ -axis:

$$\Sigma(X, Y|A, X_0, \sigma) = G(X|A, X_0, \sigma) + \Sigma_b \quad (1)$$

$$= \frac{A}{\sqrt{2\pi}\sigma} \exp\left(-\frac{1}{2}\left(\frac{X - X_0}{\sigma}\right)^2\right) + \Sigma_b.$$

$A$  denotes the amplitude of the Gaussian,  $X_0$  its center along the  $X$ -axis and  $\sigma$  its standard deviation, also along the  $X$ -axis. The probability of the model parameters  $(A, X_0, \sigma)$ , given the location  $(X_i, Y_i)$  of all considered stars in the data set, is then

$$p(A, X_0, \sigma | X_i, Y_i, \forall \text{ stars } i) \propto \mathcal{L}(X_i, Y_i, \forall \text{ stars } i | A, X_0, \sigma) p(A, X_0, \sigma), \quad (2)$$

where  $\mathcal{L}(X_i, Y_i, \forall \text{ stars } i | A, X_0, \sigma)$  is the likelihood of the model given the data points and  $p(A, X_0, \sigma)$  is the prior probability distribution for the model's parameters. The likelihood itself is the product, over all stars, of the model defined in equation (1), taken on the stellar positions. Henceforth

$$\mathcal{L}(X_i, Y_i, \forall \text{ stars } i | A, X_0, \sigma) = \prod_{\text{star } i} \Sigma(X_i, Y_i | A, X_0, \sigma)$$

$$= \prod_{\text{star } i} \left( \frac{A}{\sqrt{2\pi}\sigma} \exp\left(-\frac{1}{2}\left(\frac{X_i - X_0}{\sigma}\right)^2\right) + \Sigma_b \right) \quad (3)$$

The background density,  $\Sigma_b$  can also be expressed as a function of the model parameters by requiring that  $N_*$ , the total number of stars in the data set, corresponds to the integral of the density,  $\Sigma$ , over the field of view, of area  $\mathcal{A}$ :

$$\Sigma_b = \left( N_* - \int_{\text{FoV}} G(X|A, X_0, \sigma) dX dY \right) \mathcal{A}^{-1}. \quad (4)$$

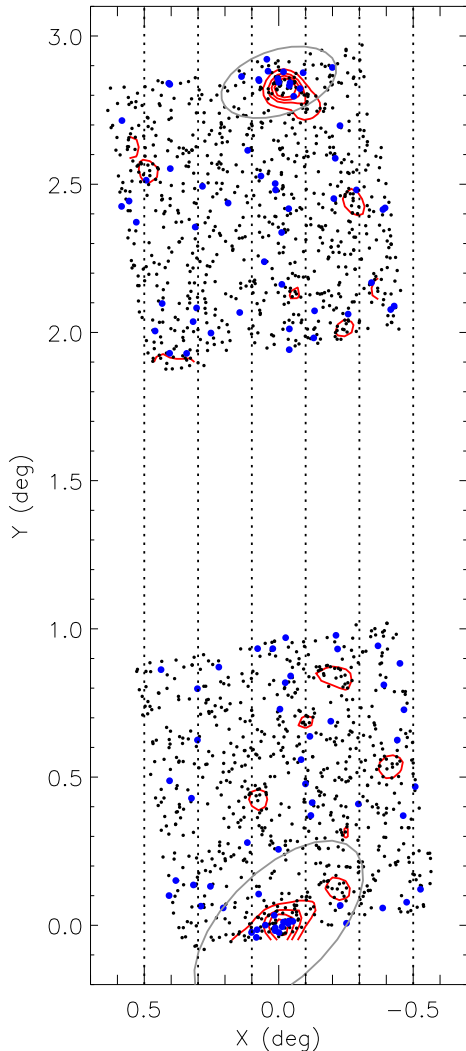


FIG. 4.— Spatial distribution of HB (blue dots) and RGB (black dots) stars around Leo IV and V, selected using the color-magnitude boxes drawn in Figure 1. The coordinates are rotated so that Leo IV and V are both at  $X = 0$  and Leo IV lies at the origin. Red contours show the RGB star density, and correspond to densities exceeding  $1.5\sigma$ ,  $3\sigma$ ,  $4\sigma$ , and  $5\sigma$  over the background density. The gray ellipses indicate the regions that are neglected when looking for extra-tidal material, and the dotted vertical lines outline the bins used for the histograms in panels (a) to (c) of Fig. 5.

The ML fits benefit from a larger sample of stars than provided by the selection boxes in Figure 1 to constrain the fit parameters optimally. Here we therefore use a different selection box (the dashed box in Figure 1) containing 5891 stars in the surveyed area but more than  $5r_h$  from the center either of the two dwarf galaxies. The prior probability distributions for the model’s parameters were chosen to be uniform over ranges that are physically motivated by a stream of stars originating from the dwarf galaxies: the probability on  $\sigma$  is uniformly distributed between  $3'$  (the typical size of the dwarf galaxies) and  $12'$ , whereas  $X_0$  and  $A$  are uniformly chosen between  $\pm 0.5^\circ$  (the width of the data set), and  $\pm 450$ , respectively. From these, we find that the most probable model has the following properties:  $X_0 = -0.13 \pm 0.03^\circ$ ,  $\sigma = 0.11 \pm 0.02^\circ$ , and  $A = 172^{+50}_{-40}$  stars/deg $^2$ . This corresponds to a back-

ground density of  $\Sigma_b = 3224$  stars/deg $^2$  for the chosen selection box and a total of 275 stars in the overdensity for the selection box and footprint used. Comparing the peak amplitude of the overdensity to the number of RGB and BHB stars in Leo IV yields a central surface brightness of  $\mu_V \simeq 32$  mag arcsec $^{-2}$ . The 2-D probability distribution functions are shown in Figure 6 for all parameters. The significance of the peak in the probability distribution function is just over  $4\sigma$  in all cases, leading us to conclude that the data show evidence of a  $4\sigma$  overdensity of stars that coincides with the bump visible in Figure 5.

## 5. DISCUSSION

All tests — the histograms in Figure 5, the KS tests and the ML fits — indicate that there is structure in the distribution of stars consistent with being Leo IV or Leo V members in the area between the systems. The strongest case is provided by the last test, which indicates a significance of the overdensity of  $\gtrsim 4\sigma$ . Aside from the preferred model, there is another local maximum visible in Figure 6 that corresponds to an underdensity in the data set. This coincides with the drop in density visible at  $X_0 \simeq +0.2^\circ$  in panels (b) and (c) of Figure 5. The limited extent of our survey perpendicular to the possible bridge of stars implies that an overdensity can also be fit as a region with high background, with an adjacent underdensity. However, marginalizing over all parameters but  $A$  (top panel of Fig. 6) makes it clear that the probability of this ‘underdensity’ is only 2%, whereas the probability of an overdensity corresponds to 98%. This shows that the structure in the field is more likely caused by an overdensity than by an underdensity. This inference is based purely on statistics, not taking into account that it is not clear what could cause an underdensity of stars in the field.

In their recent analysis, Sand et al. (2009) find no evidence for extra-tidal features emanating from Leo IV. Due to their much smaller field-of-view their analysis is, however, considerably less sensitive to the presence of a possible tidal stream, despite deeper photometry. In the region between Leo IV and Leo V, where any putative bridge would be found, our survey covers an area seven times larger than that available to Sand et al. (2009). At a given depth, this leads to a seven-fold increase in the number of stellar tracers, in our case RGB and BHB stars, that can be found. The higher sensitivity of the Sand et al. (2009) data only partly compensates for this, and only adds fainter stars in a region of the CMD where contamination by faint galaxies is high. The detection limit of Sand et al. (2009) for tidal streams of  $\mu_g \lesssim 29.8$  mag arcsec $^{-2}$  is insufficient to detect the stellar bridge, which has an estimated central surface brightness of  $\mu_V \sim 32$  mag arcsec $^{-2}$ . It is, however, interesting to note that one of the significant ‘nuggets’ of stars seen by Sand et al. (2009) to the north-west of Leo IV lies exactly on top of the location of the stellar bridge, as indicated by our ML fits.

The spatial proximity of Leo IV and Leo V and the intriguing possibility of extra-tidal material between them elicits the question of whether these two systems are somehow related and/or interacting with each other. Here we consider the following different scenarios:

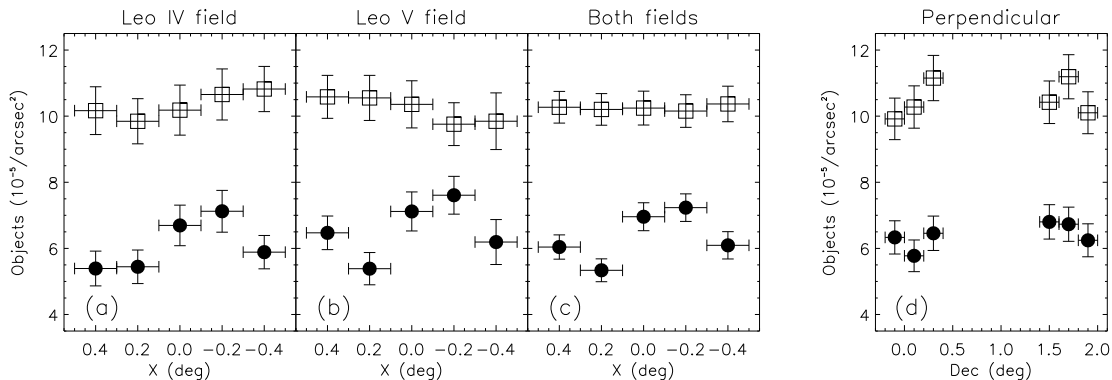


FIG. 5.— Stellar densities in  $0.2^\circ$ -wide strips. In panels (a), (b) and (c), the strips are at constant  $X$ , parallel to the straight line connecting Leo IV and V. From left to right, the panels correspond to the field containing Leo IV, the field containing Leo V, and the sum of both fields. Elliptical regions corresponding to 5 half-light radii around Leo IV and Leo V are avoided (Fig. 4). In all panels, filled circles are for stars selected with the RGB and HB color-magnitude selection boxes (Fig. 1) and open squares for foreground M dwarf stars. Vertical error bars show the Poisson errors and the horizontal error bars the width of each strip. In panel (d) the strips are at constant declination  $\delta$ , almost perpendicular to the straight line connecting Leo IV and V.

- Leo IV and Leo V might be condensations of stars in a much larger stellar stream, even though the density contrast between the condensations and the underlying stream would be very high. The apparent width of the extra-tidal substructure in the candidate RGB and HB stars of  $\sim 15$  arcmin is similar to the sizes of Leo IV and V, and is therefore consistent with this scenario. In this case they would be expected to closely follow the same orbit, which should come close enough to the Galactic center to cause the tidal disruption of a common progenitor.
- Leo IV and Leo V might have fallen into the Milky Way together as members of a group of dwarf galaxies, a process expected to be common in a  $\Lambda$ CDM cosmology (e.g. D’Onghia & Lake 2008; Li & Helmi 2008), or as satellites of a larger halo, as has been suggested for Segue 1 and 2 (Belokurov et al. 2009). Regarding the latter case, it should be noted that the revised half-light radii of Leo IV ( $\sim 200$  pc) and Leo V ( $\sim 130$  pc) make them much larger systems than Segue 1 and 2 and, in terms of size, clearly more similar to other dSphs. If they do constitute a pair with a common origin, they would still follow the same orbit around the Milky Way, but with a possibly large velocity dispersion, as they orbit a common center of mass. In this scenario, extra-tidal stars might be the result of interactions between the two galaxies, rather than with the Milky Way.
- A final option would be that Leo IV and Leo V were originally unrelated satellites of the Milky Way, but had a chance encounter. A near head-on collision might be able to cause an interaction strong enough to disrupt their stellar bodies.

### 5.1. A common orbit

If Leo IV and Leo V are tied together and follow the same orbit around the Milky Way, their common orbit should be easily determinable from simple physical arguments. In the following, we assume that the Galactocentric properties of the galaxies are interchangeable with their heliocentric properties, a reasonable assumption given the large distances to the systems compared to

the solar radius around the Milky Way. If the two dwarf galaxies lie along the same orbit, they should actually share the same orbital energy and angular momentum. The latter requirement can first be used to link together the tangential velocities of the two galaxies in the plane of the sky,  $v_{t,4}$  and  $v_{t,5}$ , and their distances,  $r_4$  and  $r_5$ , respectively for Leo IV and Leo V:  $v_{t,5} = v_{t,4}r_4/r_5$ . We then invoke energy conservation along the Leo IV/V orbit to obtain

$$(v_{\text{tot},4})^2 - (v_{\text{esc},4})^2 = (v_{\text{tot},5})^2 - (v_{\text{esc},5})^2, \quad (5)$$

where  $v_{\text{tot},i} = \sqrt{(v_{t,i})^2 + (v_{r,i})^2}$  is the total velocity of Leo  $i$ ,  $v_{r,i}$  its radial velocity with respect to the Galactic Standard of Rest, and  $v_{\text{esc},i}$  the escape velocity in the assumed model of the Milky Way potential, at the location of Leo  $i$ . For Leo IV, the tangential motion of the orbit that links Leo IV and Leo V is therefore defined by:

$$v_{t,4} = \sqrt{\left( (v_{r,5})^2 - (v_{r,4})^2 + (v_{\text{esc},4})^2 - (v_{\text{esc},5})^2 \right) \left( 1 - \left( \frac{r_4}{r_5} \right)^2 \right)^{-1}} \quad (6)$$

In order to determine  $v_{t,4}$  and  $v_{t,5}$  with their associated uncertainties, we follow a Monte Carlo scheme and randomly generate the distances and radial velocities for each of the two dwarf galaxies from Gaussian distributions defined by their observed properties, as listed in Table 2. We then determine the escape velocities required by equation (6) for the Milky Way model adopted by Paczyński (1990), after removing unphysical cases where one of the two galaxies is not bound to the Milky Way. The median and central 68.3% of the resulting distributions after 10 000 trials yield  $v_{t,4} = 239_{-6}^{+19}$  km s $^{-1}$  and  $v_{t,5} = 211_{-15}^{+30}$  km s $^{-1}$ .

These large values, combined with the small radial velocities of the dwarf galaxies, make it impossible to find a viable orbit that reproduces the observed properties of both systems at the same time. None of the orbits drawn in Figure 7 goes through both points in all panels, demonstrating that, whether Leo IV or Leo V is used as a starting point, neither the velocity nor the distance along the orbit has a strong enough gradient to replicate the observed properties of the other dwarf galaxy. This

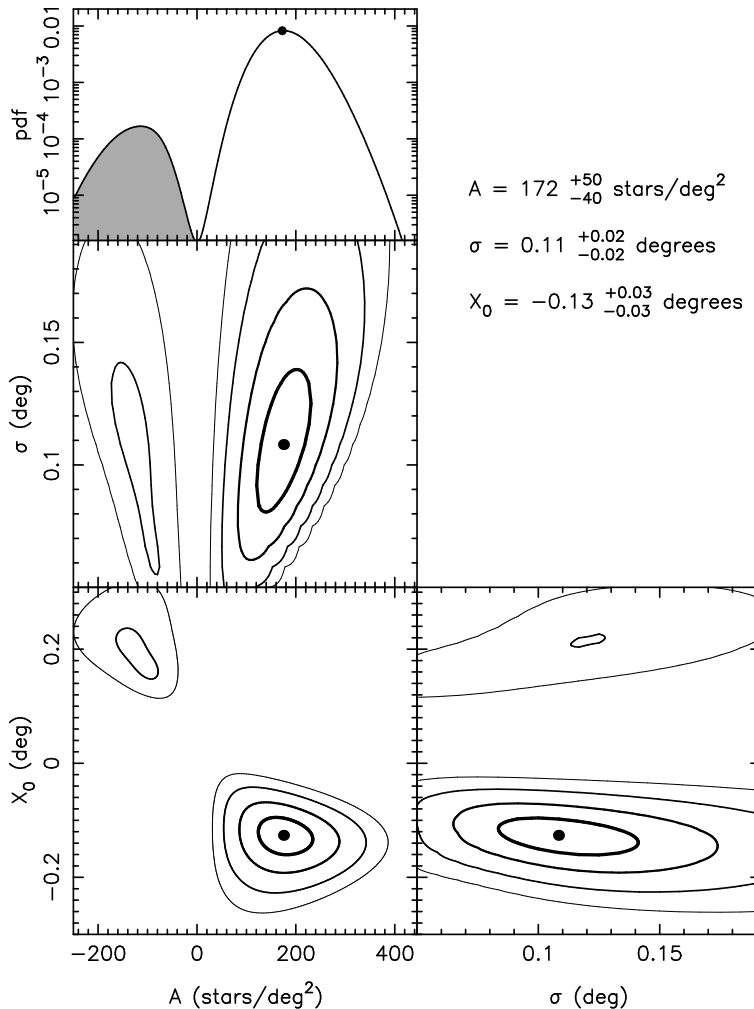


FIG. 6.— Probability distribution functions from maximum-likelihood fits of a linear Gaussian to the stellar distribution between Leo IV and Leo V. *Top panel:* probability distribution function of the model parameter  $A$  marginalized over the two other parameters. The region of negative  $A$ , shown in grey, yields a small probability of only 2%, compared to 98% for the region of positive  $A$ ; the probability of the best model (indicated with a filled circle in all panels) is a factor  $\sim 10^4$  higher than that of a uniform distribution ( $A=0$ ), which corresponds to a  $\sim 4\sigma$  significance. *Bottom panels:* for all combinations of the three fit parameters ( $A$ ,  $X_0$  and  $\sigma$ ) the two-dimensional probability function is shown, marginalized over the third parameter. Here, contours represent drops of 50%, 90%, 99% and 99.9% of the probability with respect to the best model.

analysis thus shows that Leo IV and V cannot be following the exact same orbit. We can calculate a compromise solution, with a starting point for the orbit integration that has the mean properties of the two galaxies (the central line in Figure 7). This orbit does not reproduce the velocities and distances of the two systems and remains at large Galactocentric distances, with an apocenter of 244 kpc and a pericenter of 158 kpc. We conclude that Leo IV and Leo V are very unlikely to be condensations in a larger stellar stream, for two reasons: no viable single orbit exists, and the compromise solution does not come close enough to the Galactic center for a single progenitor to have been tidally affected.

### 5.2. A ‘tumbling pair’

Rather than being remnants of a progenitor disrupted by the gravitational tides of the Milky Way, the two dwarf galaxies could be a gravitationally bound pair interacting with each other. This means that they would follow a ‘common’ orbit, but with a large velocity dispersion, as they orbit their common center of mass. Such a ‘tumbling pair’ of dwarf galaxies would be similar to the

Large and Small Magellanic Clouds, albeit much more scaled-down. For the two systems to be gravitationally bound, the total kinematic energy of the system must be less than the total gravitational potential energy. As pointed out by Davis et al. (1995), the two-body Newtonian binding criterion can be written as

$$M_{sys} \geq \frac{Rv_{los}^2}{2G \sin^2 \alpha}, \quad (7)$$

where  $M_{sys}$  is the total mass of the system,  $R$  the distance between the two objects,  $v_{los}$  the line-of-sight relative velocity, and  $\alpha$  the angle between the axis of the two-body system and the sky. Inserting the values for these parameters ( $v_{los} = 50.7 \pm 3.4$  km s $^{-1}$ ,  $R = 22 \pm 10$  kpc,  $\alpha = 70^{+6}_{-18}$ ; see Table 2 and references therein) yields a lower limit for the total mass of  $M_{sys} \geq 8 \pm 4 \times 10^9 M_{\odot}$ , or half of that for each individual dwarf.

Masses inferred from the stellar velocity dispersions in faint dSph galaxies are typically much lower, but only probe the inner few hundred parsec of their dark matter halos. Based on dynamical modeling of dSphs embedded in cosmologically motivated dark matter halos,

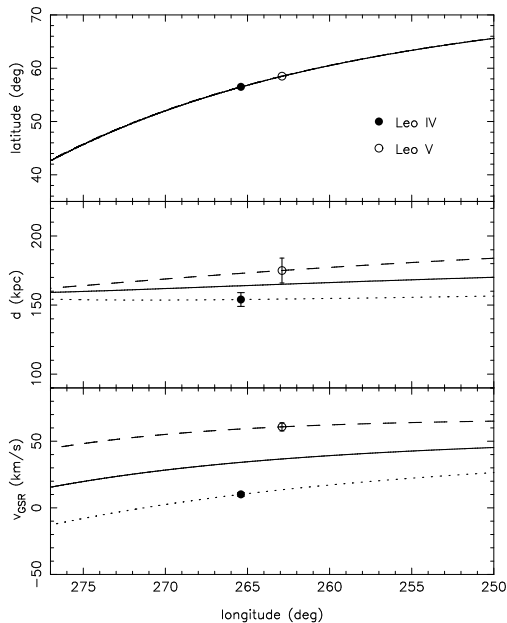


FIG. 7.— Orbits for Leo IV and V, derived assuming common energy and angular momentum for the two dwarf galaxies. The dotted, dashed and solid lines correspond to orbits with initial conditions determined using Leo IV, Leo V or their mean properties, respectively. The panels show the evolution of Galactic latitude (top), heliocentric distance (middle) and radial velocity with respect to the Galactic Standard of Rest (bottom) as functions of Galactic longitude. Properties of Leo IV and V are indicated by filled and open circles, respectively.

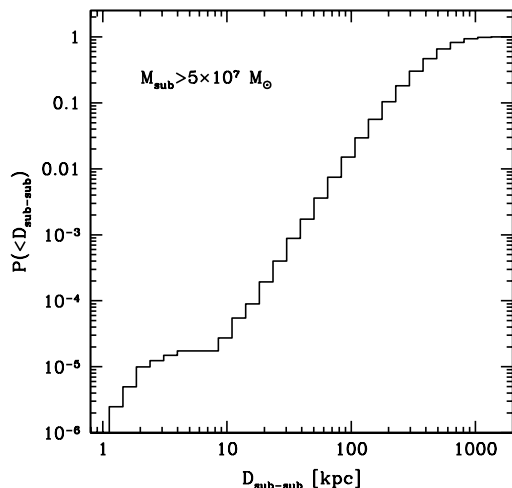


FIG. 8.— Cumulative probability distribution for the distance between two dark matter subhalos (with a current mass larger than  $5 \times 10^7 M_\odot$ ) in the last 3.4 Gyr (see text for details).

Peñarrubia et al. (2008) derive masses of up to several times  $10^9 M_\odot$  for Local Group dSphs. The masses required for Leo IV and Leo V to be a bound pair are therefore possible, but imply high mass-to-light ratios of  $M/L_V = 10^5$  in solar units.

### 5.3. A close encounter

A third option would be that Leo IV and V are unrelated systems that randomly collided in the Milky Way halo, thus provoking an interaction. Given that

the objects have a stellar extent of  $\sim 500$  pc, we estimate that they would need to come to within a few kiloparsecs of each other with a relative velocity of less than  $\sim 100 \text{ km s}^{-1}$  for tides to affect their stellar components. We used results from N-body simulations in order to compute the probability of such an encounter. We started from the four Milky Way-like dark matter ( $\Lambda$ CDM) halos presented in Macciò et al. (2009) and, for each subhalo within 250 kpc of the host galaxy’s center and with a bound mass today  $M_{\text{sub}} > 5 \times 10^7 M_\odot$ , we determined the distance to any other subhalo,  $D_{\text{sub-sub}}$ , in the last 3.4 Gyr. Figure 8 shows the cumulative probability distribution for  $D_{\text{sub-sub}}$  in the four Milky Way analogue simulations. The probability of two halos coming to within 5 kpc of one another is as low as a few times  $10^{-5}$ . In addition, this number can only be an upper limit for a galaxy-galaxy interaction, since only  $\approx 30\%$  of dark matter halos with  $M_{\text{sub}} > 5 \times 10^7 M_\odot$  are expected to host stars (Macciò et al. 2009). We conclude that a collision between Leo IV and Leo V is not a likely explanation for a possible interaction.

## 6. CONCLUSIONS

Given that Leo IV and Leo V form a close pair on the sky, in distance, and in radial velocity, it has been argued that they might be interacting or even share the same orbit (Belokurov et al. 2008). We have obtained new, deep photometry in two  $1^\circ \times 1^\circ$  fields containing both dwarf spheroidal galaxies, re-derived their structural properties, and searched for extra-tidal stars. Both Leo IV and Leo V are considerably larger than previously thought, with sizes of 206 pc and 133 pc. These sizes are similar to those of other recently discovered dSphs such as Boötes I or Ursa Major II (respectively 242 and 140 pc, Martin et al. 2008b) and the smaller ‘classical’ dSphs, for example Draco (221 pc, Martin et al. 2008b) or Leo II (185 pc, Coleman et al. 2007b). Both are also strongly elongated, with axis ratios of 2:1, which is the case for many of the fainter ( $M_V > -8$ ) dSphs (Martin et al. 2008b). We note, however, that the proximity of both dwarf galaxies near the edge of our survey might have some influence on these measurements.

The combination of deep photometry and a large area coverage of our survey provides an unprecedented sensitivity to low surface brightness features in the region between Leo IV and Leo V. Analysis of the spatial distribution of candidate RGB and HB stars using density histograms and Kolmogorov-Smirnov tests reveals the presence of a significant substructure in the observed fields. This substructure is detected at the  $\sim 3\sigma$  level, but only along the direction connecting the two systems. Maximum-likelihood modeling of the stellar distribution with a linear Gaussian confirms that the spatial structure can be fit with an overdensity connecting the two systems. With this method, the significance of the overdensity is just over  $4\sigma$ , and has a peak surface brightness of  $\mu_V \simeq 32 \text{ mag arcsec}^{-2}$ .

The reason for the close proximity of Leo IV and Leo V is still an enigma, and we have considered a few possible explanations. Orbits derived for the objects using their positions and velocities and by requiring the pair to share common values for energy and angular momentum show that it is not possible for both to be on the exact same orbit under reasonable assumptions. Furthermore, a com-



promise orbit would not approach the Galactic center closer than  $\sim 160$  kpc, as also noted by Belokurov et al. (2008). Hence, it is highly unlikely that Leo IV and Leo V are condensations in a low surface brightness stellar stream resulting from the tidal disruption of a common progenitor. The fact that the elongations of the two systems are not aligned might be a further indication of this. A large velocity dispersion around a mutual orbit, for example in the case of a ‘tumbling pair’ of dwarf galaxies, is only viable if Leo IV and Leo V have masses of at least a few times  $10^9 M_{\odot}$ . This would imply extreme V-band mass-to-light ratios of  $\gtrsim 10^5$  in solar units, but recent dynamical simulations of dwarf spheroidal galaxies (Peñarrubia et al. 2008) show that the required masses are possible. If Leo IV and Leo V are indeed a bound and internally interacting pair, this could account naturally for their unaligned elongations and the offset of the apparent ‘stellar bridge’ from the straight line connecting

them. Finally, analysis of Milky Way-like  $\Lambda$ CDM halos reveals that the probability of two satellites colliding is negligibly small. This is consistent with the findings of Belokurov et al. (2008) who calculate a  $\lesssim 1\%$  probability for such a close association happening by chance. Therefore, the scenario in which Leo IV and Leo V are a bound pair of dwarf galaxies, orbiting and interacting with each other, appears to be the most viable explanation for this close celestial companionship.

The authors thank the anonymous referee for helpful comments. Based on observations collected at the Centro Astronómico Hispano Alemán (CAHA) at Calar Alto, operated jointly by the Max-Planck Institut für Astronomie and the Instituto de Astrofísica de Andalucía (CSIC). This research has made use of the Vizier catalogue access tool, CDS, Strasbourg, France.

## REFERENCES

- Abazajian, K. N., Adelman-McCarthy, J. K., Agüeros, M. A., Allam, S. S., Allende Prieto, C., et al. 2009, *ApJS*, 182, 543  
 Belokurov, V., Zucker, D. B., Evans, N. W., Kleyana, J. T., Koposov, S., et al. 2007, *ApJ*, 654, 897  
 Belokurov, V., Walker, M. G., Evans, N. W., Faria, D. C., Gilmore, G., et al. 2008, *ApJ*, 686, L83  
 Belokurov, V., Walker, M. G., Evans, N. W., Gilmore, G., Irwin, M. J., et al. 2009, arXiv:0903.0818  
 Bertin, E., & Arnouts, S. 1996, *A&AS*, 117, 393  
 Bertin, E. 2006, in *Astronomical Data Analysis Software and Systems XV*, ASP Conf. Series 351, 112  
 Coleman, M. G., de Jong, J. T. A., Martin, N. F., Rix, H.-W., et al. 2007a, *ApJ*, 668, L43  
 Coleman, M. G., Jordi, K., Rix, H.-W., Grebel, E. K. & Koch, A. 2007b, *AJ*, 134, 1938  
 Davis, D. S., Bird, C. M., Moshotzky, R. F. & Odewahn, S. C. 1995, *ApJ*, 440, 48  
 de Jong, J. T. A., Rix, H.-W., Martin, N. F., et al. 2008a, *AJ*, 135, 1361  
 de Jong, J. T. A., Harris, J., Coleman, M. G., Bell, E. F., Rix, H.-W., et al. 2008b, *ApJ*, 680, 1112  
 D’Onghia, E. & Lake, G. 2008, *ApJ*, 686, L61  
 Dotter, A., Chaboyer, B., Jevremović, D., Baron, E., Ferguson, J. W., Sarajedini, A. & Anderson, J. 2007, *AJ*, 134, 376  
 Dotter, A., Chaboyer, B., Jevremović, D., Kostov, V., Baron, E. & Ferguson, J. W. 2008, *ApJS*, 178, 89  
 Gilmore, G., Wilkinson, M. I., Wyse, R. F. G., Kleyana, J. T., Koch, A., Evans, N. W. & Grebel, E. K. 2007, *ApJ*, 663, 948  
 Jester, S., Schneider, D. P., Richards, G. T., Green, R. F., Schmidt, M., et al. 2005, *AJ*, 130, 873  
 Koposov, S. E., Belokurov, V., Evans, N. W., Hewett, P. C., Irwin, M. J., et al. 2008, *ApJ*, 686, 279  
 Koposov, S. E., Yoo, J., Rix, H.-W., Weinberg, D. H., Macciò, A. V. & Escudé, J. M. 2009, *ApJ*, 696, 2179  
 Li, Y.-S. & Helmi, A. 2008, *MNRAS*, 385, 1365  
 Lynden-Bell, D. & Lynden-Bell, R. M. 1995, *MNRAS*, 275, 429  
 Macciò, A. V., Kang, X., Fontanot, F., Somerville, R. S., Koposov, S. E. & Monaco, P. 2009, arXiv:0903.4681  
 Martin, N. F., Ibata, R. A., Chapman, S. C., Irwin, M. & Lewis, G. F. 2007, *MNRAS*, 380, 281  
 Martin, N. F., Coleman, M. G., de Jong, J. T. A., Rix, H.-W., et al. 2008a, *ApJ*, 672, L13  
 Martin, N. F., de Jong, J. T. A. & Rix, H.-W., 2008b, *ApJ*, 684, 1075  
 Martin, N. F., McConnachie, A. W., Irwin, M., Widrow, L. M., Ferguson, A. M. N. et al. 2009, in press, arXiv:0909.0399  
 Moretti, M. I., Dall’Ora, M., Ripepi, V., Clementini, G., Di Fabrizio, L., et al. 2009, *ApJ*, 699, L125  
 Paczyński, B. 1990, *ApJ*, 348, 485  
 Peñarrubia, J., McConnachie, A. W. & Navarro, J. F. 2008, *ApJ*, 672, 904  
 Press, W.H., Teukolsky, S.A., Vetterling, W.T., Flannery, B.P. 1992, *Numerical recipes in C. The art of scientific computing*. Cambridge: University Press, 1992, 2nd ed.  
 Sand, D. J., Set, A., Olszewski, E. W., Willman, B., Zaritsky, D. & Kallivayalil, N. 2009, *ApJ*, *subm.*, arXiv:0911.5352  
 Schlegel, D., Finkbeiner, D. & Davis, M. 1998, *ApJ*, 500, 525  
 Simon, J. & Geha, M. 2007, *ApJ*, 670, 313  
 Walker, M. G., Belokurov, V., Evans, N. W., Irwin, M. J., Mateo, M., Olszewski, E. W. & Gilmore, G. 2009, *ApJ*, 694, L144